

A Monolithic All-Optical Push–Pull Wavelength Converter

Joseph A. Summers, *Student Member, IEEE*, Milan L. Mašanović, *Member, IEEE*, Vikrant Lal, *Member, IEEE*, and Daniel J. Blumenthal, *Fellow, IEEE*

Abstract—We present the first two-stage all-optical push–pull wavelength converter, which has been monolithically integrated in indium phosphide, using an offset quantum-well platform. The device incorporates two cascaded wavelength converters, each with an integrated tunable sampled-grating distributed Bragg reflector laser, and deeply etched total internal reflection mirrors for a compact layout. The device, under push–pull operation, is demonstrated to reduce converted signal pattern dependence at 10 Gb/s, while providing improved phase swing compared to previous offset quantum-well designs. The device is shown to achieve full π phase swing in the second-stage wavelength converter over a 12-dB input power range.

Index Terms—Mach–Zehnder interferometer (MZI), photonic integrated circuits, total internal reflection (TIR) mirror, tunable laser, wavelength conversion, wavelength converter.

I. INTRODUCTION

THE semiconductor-optical-amplifier-based Mach–Zehnder interferometer (SOA-MZI) has emerged as a preeminent technology for photonic integrated circuits, particularly for all-optical wavelength conversion, digital logic, and signal regeneration [1]–[3]. This popularity is due in part to the SOA-MZI’s fast speed and potential for monolithic integration on chip with a variety of active and passive optical components, such as lasers, routers, and electrooptic modulators [3]–[5].

The switching operation of an SOA-MZI is driven by carrier-induced phase shift in one or both MZI arms, resulting from amplification of an input optical signal in the SOA. As such, the amount of phase shift in an SOA-MZI arm is determined by the linewidth enhancement factor, the input optical power, the length of the SOA, and the overlap between the optical mode and the active regions. For a given active material, the optical mode overlap, or confinement factor, can vary significantly between different active–passive integration platforms. This results in a range of cross-phase-modulation (XPM) efficiencies and for certain integration platforms, such as offset quantum-well platforms, a low confinement factor ($\sim 7\%$) makes full π phase swing in the SOA-MZI difficult to attain [6]. Improvement in phase swing can be made by amplifying the signal going into the MZI, but this comes at the expense of greater noise, as well as saturation and pattern dependence.

Manuscript received May 29, 2007; revised July 12, 2007. This work was supported by the Defense Advanced Research Projects Agency (DARPA)/MTO CS-WDM and SPAWAR Program under Grant N66001-02-C-8026.

The authors are with the Electrical and Computer Engineering Department, University of California Santa Barbara, Santa Barbara, CA 93106 USA (e-mail: jsummers@ece.ucsb.edu).

Digital Object Identifier 10.1109/LPT.2007.906846

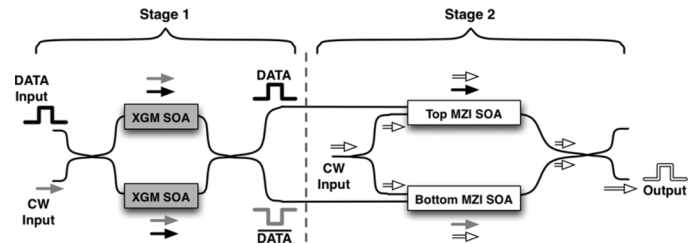


Fig. 1. Schematic illustrating the principles of all-optical push–pull wavelength conversion, implemented using two cascaded wavelength converters.

Alternatively, the phase swing of an SOA-MZI can be improved by operating in push–pull mode, which involves simultaneously pumping the phase of both arms in opposite directions with complementary optical input signals (DATA , $\overline{\text{DATA}}$). Such push–pull operation has been demonstrated, using two externally modulated inputs, to improve the output signal-to-noise ratio and the extinction ratio [7]. In order for this approach to be practical, however, both DATA and $\overline{\text{DATA}}$ must be generated using a single optical input.

In this letter, we report on a monolithic all-optical push–pull wavelength converter that operates using a single optical input. The design consists of two cascaded wavelength conversion stages, each consisting of an integrated tunable probe laser. The first stage uses the input DATA to generate a $\overline{\text{DATA}}$ signal, and then spatially separates the two signals to operate the second SOA-MZI stage in push–pull mode.

Static measurements demonstrate full π phase swing, while 10-Gb/s eye diagrams and bit-error-rate (BER) measurements show noticeable improvement in pattern dependence and extinction ratio by operating the device in push–pull mode.

II. PRINCIPLES OF PUSH–PULL OPERATION

Unlike conventional SOA-MZI operation where only a single arm is pumped [1], push–pull operation entails simultaneous pumping of both SOA-MZI arms with opposite polarity signals (DATA , $\overline{\text{DATA}}$). This dual pumping modulates the carrier density and phase of the SOA-MZI arms in opposite directions (aka “push–pull”), which results in greater overall interferometer phase swing.

Practical implementation of a push–pull SOA-MZI requires that two synchronous, complementary pump signals be generated from a single optical input signal. This is accomplished in this work using a two-stage wavelength conversion scheme (Fig. 1). In the first stage, a single input DATA signal is used to create an inverted signal ($\overline{\text{DATA}}$) through cross-gain modulation (XGM) of a continuous-wave (CW) probe. The DATA and $\overline{\text{DATA}}$ signals are then routed to separate ports at the output

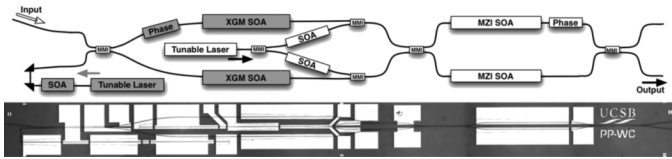


Fig. 2. (top) Schematic of the all-optical push-pull wavelength converter design, and (bottom) a composite microscope image of the fabricated device.

of the first stage, and fed into the two arms of the second-stage SOA-MZI for push-pull operation.

In order to simultaneously perform wavelength conversion and signal separation between DATA and $\overline{\text{DATA}}$, the first stage utilizes a parallel SOA structure [8]. Here, the input DATA pump signal and a CW probe signal are split evenly between two symmetric XGM SOAs. Within the XGM SOA of each arm, the DATA signal is encoded onto the probe signal through XGM, producing DATA and $\overline{\text{DATA}}$ signals at the output of each arm. If the XGM SOAs are operated symmetrically, then at the output of each XGM SOA the signals in the two arms will be equal in amplitude but out of phase by $\pi/2$. When the two arms are combined at the output of the first stage, another $\pi/2$ phase shift is introduced and the DATA and $\overline{\text{DATA}}$ signals are routed to opposite ports. These outputs, which are aligned in time, then feed into opposite arms of the second-stage SOA-MZI.

III. DEVICE DESIGN

The push-pull wavelength converter was fabricated in InP, using an offset quantum-well platform [3], and measures $0.6 \text{ mm} \times 7.0 \text{ mm}$. A schematic and a composite microscope image of the device are provided in Fig. 2.

The push-pull wavelength converter design includes two tunable sampled-grating distributed Bragg reflector (SG-DBR) lasers that provide an integrated probe signal for each wavelength converter stage. SOAs after each probe laser provide amplification and, in the case of the second-stage laser, power balance between the two arms of the SOA-MZI. In order to reduce the overall length of the design, the first wavelength converter stage is folded, such that the first-stage SG-DBR probe laser lies adjacent to the arms of the XGM SOA structure. The probe signal is then sharply redirected into the first stage using two deeply etched 90° TIR corner mirrors [9]. In contrast to the two-stage design depicted in Fig. 1, the output multimode interference coupler of the first XGM stage is shared by the second-stage SG-DBR probe laser. This allows the XGM SOAs to be placed adjacent to the second-stage probe laser, such that introduction of the first-stage XGM converter does not significantly add to the overall length of the device. Phase electrodes in the arms of each stage are used to maximize DATA and $\overline{\text{DATA}}$ signal separation (first stage) and converted signal extinction ratio (second stage).

IV. EXPERIMENT AND RESULTS

The device was tested to determine static XPM efficiency and dynamic wavelength conversion performance at 10-Gb/s nonreturn-to-zero. A schematic of the experimental setup is shown in Fig. 3.

The input pump signal was provided by an external CW laser, which was encoded with data using an electrooptic modulator. An erbium-doped fiber amplifier (EDFA) was placed after the

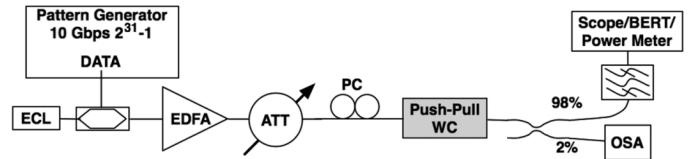


Fig. 3. Schematic of experimental setup.

modulator to boost signal power, and a variable optical attenuator provided control of the power going into the device. Due to the polarization sensitivity of quantum-well active regions, a polarization controller (PC) was required to adjust the input signal polarization to transverse electric (TE). The input and output signals were coupled to and from the device using lensed fibers. The output signal was passed through a fused fiber tap, with 2% of the signal going to an optical spectrum analyzer (OSA) for continuous monitoring of the output spectrum. The remaining 98% was passed through a tunable bandpass filter, and was used to measure output signal power, eye diagrams, or take BER measurements. The device, which was soldered onto a copper bar, was probed directly with dc needles probes and maintained at 17°C throughout testing.

For all experiments, the MZI SOAs (length = 1 mm) were operated at 300 mA, and the XGM SOAs (length = 1 mm) were operated at 250 mA. The following steps were taken in order to maximize signal separation between DATA and $\overline{\text{DATA}}$ going into the SOA-MZI. First, the external pump and the second-stage probe laser signals were turned OFF. Next, the power from the first-stage probe laser was absorbed and monitored in both of the SOA-MZI arms, by reverse biasing the MZI SOAs and measuring the photocurrent. Finally, the first-stage phase electrode current was adjusted to maximize the difference in photocurrent between the two SOA-MZI arms. A maximum signal separation of 14 dB was measured using photocurrent, and confirmed by forward-biasing the bottom MZI SOA and monitoring the output. This also showed approximately 12 dB of crosstalk between DATA and $\overline{\text{DATA}}$. Once the first-stage operating parameters were determined, the input pump signal and second-stage probe laser were turned back ON and the device was operated as normal.

The XPM efficiency of the push-pull wavelength converter was determined using techniques described in detail here [6]. First, the data signal going to the input pump was turned OFF to provide an input CW signal. The input pump power was then adjusted using the variable optical attenuator, and for each input power, the phase electrode current of the SOA-MZI was swept. This produced a family of MZI phase transfer functions, measured at the output of the device by an optical power meter, using the filtered signal from second-stage probe. The SOA-MZI XPM efficiency was then determined using the shift in the transfer function over the range of input powers. XPM efficiency measurements were made for four different first-stage probe powers (Fig. 5).

The XPM efficiency measurements show that, with the first-stage probe OFF, the XGM SOA structure is able to provide sufficient gain to the pump signal to achieve more than 2π of phase swing in the SOA-MZI (over a 30-dB input power range). However, corresponding eye-diagram measurements for the wavelength converted signal show significant pattern dependence using the same peak pump power ($= 2 \text{ dBm}$), due

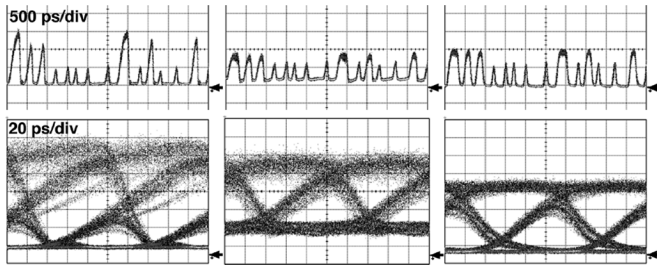


Fig. 4. The 10-Gb/s converted patterns and eye diagrams with (left) XGM probe OFF, MZI phase adjusted to minimize “0” power level, (center) XGM probe OFF, MZI phase adjusted to minimize pattern dependence, and (right) XGM probe ON (= 0 dBm).

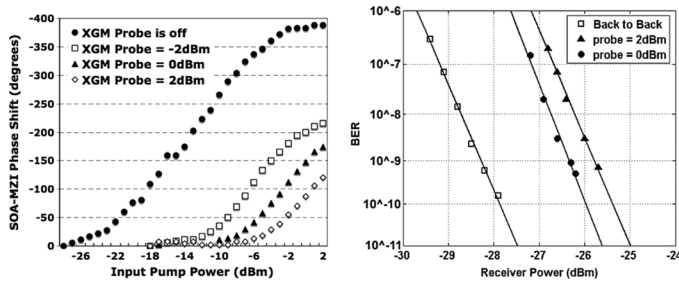


Fig. 5. (left) Phase shift in the SOA-MZI as a function of input power for the push-pull wavelength converter, (right) 10-Gb/s BER measurements for push-pull wavelength conversion with two different first-stage probe powers.

to SOA saturation and slow gain recovery ($\tau_t \sim 150$ ps) [Fig. 4 (left)]. This pattern dependence can be partially mitigated by adjusting the MZI phase electrode [Fig. 4 (center)], but this comes at the expense of reduced extinction ratio (≈ 6 dB), and for both cases, the signal is not error-free [10].

When the first-stage probe laser (power = 0 dBm) is turned ON for push-pull operation, eye-diagrams show significant improvement in pattern dependence and extinction ratio (≈ 12 dB) with error-free operation (Fig. 5). Improvement in pattern dependence can be attributed to power equalization in the MZI SOAs due to the finite signal separation of DATA and $\overline{\text{DATA}}$ [11]. Increasing the first-stage probe power beyond 0 dBm further reduces the pattern dependence, but also reduces the first-stage XGM efficiency and output extinction ratio, causing an increase in power penalty. Phase measurements for push-pull show an increase in input saturation power, while still allowing a full π phase swing over an input power range of 12 dB. This is twice the phase swing than has previously been reported in the offset quantum-well platform, over the same input power range [6].

V. SUMMARY AND CONCLUSION

This letter reported on the design and testing of a novel two-stage all-optical push-pull wavelength converter. The design successfully integrated two SG-DBR lasers, operating

simultaneously, with TIR corner mirrors to fold the device for a compact layout. The cascaded push-pull wavelength conversion scheme was demonstrated to improve converted signal pattern dependence at 10 Gb/s, while achieving full π phase swing in the second stage of the device. This phase performance is twice that of previous, single-stage devices fabricated in the same offset quantum-well integration platform. Future devices will aim to improve the SOA gain recovery through lower active region temperatures (better electrical contact) or use of hybrid active platforms (e.g., [5]).

All-optical push-pull operation of SOA-MZIs is a promising approach to improving the efficiency of SOA-based switches, with the potential for better performance and shorter interaction length. Through use of an inverted signal generated on-chip, the performance of cascaded optical switches may also be improved.

REFERENCES

- [1] T. Durhuus, C. Joergensen, B. Mikkelsen, R. J. S. Pedersen, and K. E. Stubkjaer, “All-optical wavelength conversion by SOA’s in Mach-Zehnder configuration,” *IEEE Photon. Technol. Lett.*, vol. 6, no. 1, pp. 53–55, Jan. 1994.
- [2] J.-Y. Kim, J.-M. Kang, T.-Y. Kim, and S.-K. Han, “All-optical multiple logic gates with XOR, NOR, OR, and NAND functions using parallel SOA-MZI structures: Theory and experiment,” *J. Lightw. Technol.*, vol. 24, no. 9, pp. 3392–3399, Sep. 2006.
- [3] M. L. Mašanović, V. Lal, J. A. Summers, J. S. Barton, E. J. Skogen, L. G. Rau, L. A. Coldren, and D. J. Blumenthal, “Widely tunable monolithically integrated all-optical wavelength converters in InP,” *J. Lightw. Technol.*, vol. 23, no. 3, pp. 1350–1362, Mar. 2005.
- [4] P. Bernasconi, L. Zhang, W. Yang, N. Sauer, L. L. Buhl, J. H. Sinsky, I. Kang, S. Chandrasekhar, and D. T. Neilson, “Monolithically integrated 40-Gb/s switchable wavelength converter,” *J. Lightw. Technol.*, vol. 24, no. 1, pp. 71–76, Jan. 2006.
- [5] V. Lal, M. L. Mašanović, J. A. Summers, and D. J. Blumenthal, “Monolithic wavelength converters for high-speed packet-switched optical networks,” *IEEE J. Sel. Topics Quantum Electron.*, vol. 13, no. 1, pp. 49–57, Jan./Feb. 2007.
- [6] M. L. Mašanović, V. Lal, E. J. Skogen, J. S. Barton, J. A. Summers, J. A. Raring, L. A. Coldren, and D. J. Blumenthal, “Cross-phase modulation efficiency in offset quantum-well and centered quantum-well semiconductor optical amplifiers,” *IEEE Photon. Technol. Lett.*, vol. 17, no. 11, pp. 2364–2366, Nov. 2005.
- [7] J. A. Summers, M. L. Mašanović, V. Lal, and D. J. Blumenthal, “Monolithic spatially-filtered 10 Gbps all-optical wavelength converter with enhanced push-pull operation using dual inverted and non-inverted inputs,” in *Proc. IEEE/OSA Opt. Fiber Commun. Conf.*, Anaheim, CA, Mar. 5–10, 2006.
- [8] J. Leuthold, P.-A. Besse, E. Gamper, M. Dülk, S. Fischer, G. Guekos, and H. Melchior, “All-optical Mach-Zehnder interferometer wavelength converters and switches with integrated data- and control-signal separation scheme,” *J. Lightw. Technol.*, vol. 17, no. 6, pp. 1056–1066, Jun. 1999.
- [9] H. Appelman, J. Levy, M. Pion, D. Krebs, C. Harding, and M. Zediker, “Self-aligned chemically assisted ion-beam-etched GaAs/(Al,Ga)As turning mirrors for photonic applications,” *J. Lightw. Technol.*, vol. 8, no. 1, pp. 39–41, Jan. 1990.
- [10] J. A. Summers, M. L. Mašanović, V. Lal, and D. J. Blumenthal, “Monolithically integrated multi-stage all-optical 10 Gbps push-pull wavelength converter,” in *Proc. IEEE/OSA Opt. Fiber Commun. Conf.*, Anaheim, CA, Mar. 25–29, 2007, to be published.
- [11] S. Bischoff, M. L. Nielsen, and J. Mørk, “Improving the all-optical response of SOAs using a modulated holding signal,” *J. Lightw. Technol.*, vol. 22, no. 5, pp. 1303–1308, May 2004.